

2025

Synthesis and Luminescence Dynamics of CdSe and CdSe/CdS Quantum Dots

Asset Zh. Kainarbay

Faculty of Physics and Technical Sciences, L.N. Gumilyov Eurasian National University, Astana 010008, Kazakhstan, kainarbai_azh@enu.kz

Aigerim K. Ospanova

Faculty of Physics and Technical Sciences, L.N. Gumilyov Eurasian National University, Astana 010008, Kazakhstan

Zhakyp T. Karipbayev

Faculty of Physics and Technical Sciences, L.N. Gumilyov Eurasian National University, Astana 010008, Kazakhstan

Raigul N. Kassymkhanova

Faculty of Physics and Technical Sciences, L.N. Gumilyov Eurasian National University, Astana 010008, Kazakhstan

Aizhan S. Akhmetova

Faculty of Physics and Technical Sciences, L.N. Gumilyov Eurasian National University, Astana 010008, Kazakhstan

Follow this and additional works at: <https://www.ephys.kz/journal>

See next page for additional authors

Recommended Citation

Kainarbay, Asset Zh.; Ospanova, Aigerim K.; Karipbayev, Zhakyp T.; Kassymkhanova, Raigul N.; Akhmetova, Aizhan S.; Yussupbekova, Bagila N.; Alibay, Temirlan T.; Zhangylyssov, Keleshek B.; and Sarsenova, Zarina (2025) "Synthesis and Luminescence Dynamics of CdSe and CdSe/CdS Quantum Dots," *Eurasian Journal of Physics and Functional Materials*: Vol. 9: No. 3, Article 1.

DOI: <https://doi.org/10.69912/2616-8537.1247>

This Review is brought to you for free and open access by Eurasian Journal of Physics and Functional Materials. It has been accepted for inclusion in Eurasian Journal of Physics and Functional Materials by an authorized editor of Eurasian Journal of Physics and Functional Materials.

Synthesis and Luminescence Dynamics of CdSe and CdSe/CdS Quantum Dots

Authors

Asset Zh. Kainarbay, Aigerim K. Ospanova, Zhakyp T. Karipbayev, Raigul N. Kassymkhanova, Aizhan S. Akhmetova, Bagila N. Yussupbekova, Temirlan T. Alibay, Keleshek B. Zhangylyssov, and Zarina Sarsenova

REVIEW

Synthesis and Luminescence Dynamics of CdSe and CdSe/CdS Quantum Dots

Asset Z. Kainarbay^{*}, Aigerim K. Ospanova^{**}, Zhakyp T. Karipbayev, Raigul N. Kassymkhanova, Aizhan S. Akhmetova, Bagila N. Yussupbekova, Temirlan T. Alibay, Keleshek B. Zhangylyssov, Zarina Sarsenova

Faculty of Physics and Technical Sciences, L.N. Gumilyov Eurasian National University, Astana 010008, Kazakhstan

Abstract

The aim of the study is to analyze the luminescent properties of hexagonal quantum dots and their bridged envelope compounds under constant and temporal spectral analysis conditions. The CdSe nanoparticles were obtained by the hot injection method. To increase the radiation efficiency, CdSe/CdS core-shell structures have been synthesized, ensuring the passivation of surface defects. Steady-state optical measurements have shown that the first absorption maximum is recorded at 546.48 nm (2.26 eV), while the photoluminescence peak falls to 565.89 nm (2.19 eV). The data obtained indicate the presence of a Stokes shift of approximately 70 meV with a quantum radiation power of 21.4 %. The time-resolved luminescence has three attenuation components with lifetimes of 7, 25 and 54 ns, which gives an average value of 26 ns. For CdSe/CdS nanoparticles, a noticeable increase in the lifetime of excited states is observed — up to 103 ns, which is probably due to the stabilizing effect of the polymer medium on the surface of the quantum dots. A long-wavelength peak at 742 nm exhibited a prolonged relaxation component of ~1.033 μ s, associated with structural defects in the crystal lattice. These findings highlight the critical role of synthesis parameters and surface modifications in optimizing the luminescent properties of quantum dots for various applications.

Keywords: CdSe, Nanoparticles, Luminescence, Time-resolved luminescence

1. Introduction

In recent years, metal nanocrystals and semiconductor-nanoparticles with characteristic physical and chemical properties - have become promising materials for use in various advanced technologies.

Its applications cover a variety of fields, including solar energy recovery, the development of photo-electronic components, high-resolution molecular and cellular imaging and ultra-sensitive detection technologies [1–3].

Nanocrystals of fluorescent semiconductors, in particular cadmium selenide quantum dots (CdSe), have become very attractive in recent years due to their exceptional optical properties. Its attractiveness lies, for example, in the adjustable band gap (E_g), impressive quantum efficiency (QY) and the

possibility of complex surface treatment, which opens up wide opportunities in optoelectronics, bioimaging and nanotechnology [4,5]. These characteristics, combined with their nanoscale dimensions and versatile applications, make QDs indispensable in optoelectronics, bioimaging, and display technologies. In addition, coating CdSe quantum dots with a thin semiconductor layer with a wider band gap, such as cadmium sulfide (CdS) or zinc sulfide (ZnS), significantly improves their luminescence. This enhancement is attributed to the elimination of surface traps, such as selenium-hole defects, through effective surface passivation [6–10]. CdSe/CdS core/shell nanocrystals are particularly noteworthy for their superior emission characteristics, which are observable both at the single-dot level and in ensemble studies [11].

Received 12 May 2025; revised 5 June 2025; accepted 6 June 2025.
Available online 7 October 2025

* Corresponding author.

** Corresponding author.

E-mail addresses: kainarbai_azh@enu.kz (A.Z. Kainarbay), aygerim-ospanova-00@mail.ru (A.K. Ospanova).

<https://doi.org/10.69912/2616-8537.1247>

2616-8537/© 2025 L.N. Gumilyov Eurasian National University. This is an open access article under the CC BY 4.0 DEED Attribution 4.0 International (<https://creativecommons.org/licenses/by/4.0/>).

Colloidal QDs are typically coated with organic ligands, which play multifaceted roles. These ligands not only ensure colloidal stability and facilitate integration into matrices (a process known as QD functionalization) but also influence exciton dynamics, passivate surface defects, and modify electron transport properties in QD films [12,13]. The choice of organic ligands significantly impacts the luminescent properties of QDs, as their electrochemical properties determine the degree of luminescence enhancement or quenching. For instance, ligand substitution can either quench or enhance luminescence [13], and replacing a single ligand with a ligand complex has been reported to dramatically increase the QY [14–17]. Despite these advancements, the intrinsic QY of bare CdSe cores remains low, typically ranging from 0.1 % to 1.5 %. The research conducted by the authors covered a wide range of parameters of quantum dot synthesis, including temperature, process duration, and the ratio between cadmium and selenium precursors, in order to determine their effect on quantum yield (QY). Mixtures of coordinating solvents such as TOPO (tri-*n*-octylphosphinoxide), HDA (hexadecylamine), and TOP (tri-*n*-octylphosphine) were often used during synthesis to regulate the rate of nanoparticle formation and prevent the Ostwald maturation effect. For instance, studies [14,15] have demonstrated that this stabilizer composition enables the achievement of a high QY (50–90 %).

Advances in colloidal synthesis techniques have facilitated the production of QDs with diverse chemical compositions, sizes, shapes, and surface functionalization, allowing their integration into various matrices and the development of QD-based devices [18–20]. The efficiency of quantum dots largely depends on their surface properties and structural mobility, therefore, a detailed study of the interactions between organic ligands and nanoparticles plays a key role in optimizing the characteristics of optoelectronic composites [7].

Despite notable successes in the study of the luminescent characteristics of CdSe quantum dots, there are still a number of unresolved scientific problems in this field. For instance, while the role of surface properties in influencing luminescence has been explored [4], the precise relationship between surface quality and nanoparticle growth dynamics is yet to be fully understood. Additionally, the synthesis parameters, such as temperature, time, and cadmium-to-selenium precursor ratios, have been shown to critically affect QD QY [15]. Despite these findings, gaps persist in quantitatively correlating synthesis conditions with photophysical properties.

Furthermore, the integration of QDs into advanced lighting technologies highlights the need for a deeper

understanding of the theoretical underpinnings and experimental results. Specifically, the quantitative description of time-resolved photoluminescence decay spectra remains a topic requiring further investigation [20].

In this study, various types of QD samples, including CdSe and CdSe/CdS, modified with functional ligands such as oleic acid and an HDA + TOPO + TOP mixture, were synthesized. A nanocomposite based on CdSe QDs was also fabricated. The time-resolved and spatially-resolved luminescent properties of these colloidal QDs, incorporating different structures and surface modifications, were systematically studied at room temperature. To study the optical properties in detail, studies were carried out using various spectroscopic methods: analysis of absorption spectra, photoluminescence in stationary and temporary modes, as well as X-ray luminescence.

2. Material and methods

Optical absorption spectra in the range from 200 to 1200 nm were measured in the ultraviolet and visible regions using a Jasco V770 spectrophotometer. Photoluminescence (PL), excitation spectra measurements in visible region investigated using the spectrofluorimeter SM2203.

The luminescence of the studied samples was excited using various methods. For photoluminescence (PL) measurements, two excitation sources were used: a xenon lamp with a wavelength range of 200–850 nm and a pulsed laser with a wavelength of 450 nm and a pulse duration of 5–10 ns. Measurements were carried out at a temperature of 300 K. X-ray luminescence (XRL) was recorded under X-ray irradiation generated by a tungsten X-ray tube operating at 30 keV and 10 mA, also at 300 K.

Time-resolved spectroscopy was employed to analyze the luminescence spectra over a time window ranging from 10^{-8} to 10^{-3} s, using nanosecond-scale delays at a constant temperature of 300 K. Photoluminescence (PL) excitation was carried out with two systems: the Ekspla NT 342/3UV, offering 5 ns pulse durations across the 220–1100 nm range, and the Solar LQ215 combined with LP603 and LG350, delivering 10 ns pulses within the broader 210–2500 nm spectral range. Excitation and emission spectra were recorded using a Solar CM2203 fluorescence spectrophotometer, which employs a xenon lamp as the excitation source. For X-ray luminescence (XRL) measurements, an Andor Shamrock B303i spectrometer equipped with a DU-401A-BV CCD camera was used to capture data in the energy range of 1.0–3.4 eV. It is worth emphasizing that different spectrometers and excitation systems were used for PL

and XRL measurements, which should be taken into account when comparing the spectra.

2.1. Sample preparation

Established synthesis methods with minor modifications were employed to prepare the quantum dot (QD) samples. No further purification of the purchased reagents was undertaken. Quantum dots (QDs) were synthesized with the goal of achieving strong luminescence in the red and near-infrared (NIR) regions. Their excitation was specifically carried out using intense ultraviolet (UV) light to stimulate emission within the targeted spectral range. The synthesized samples are hereafter referred to as QDs. For all QDs, the synthesis duration was standardized at 5 min, which was determined to yield the maximum intensity of the excitonic photoluminescence band.

2.1.1. $\mathcal{N}\ominus 1$ QDs (CdSe/CdS-Cu(1 %))

The copper-doped samples were synthesized according to the authors' method [21,22]. The method of hot injection from pre-synthesized cadmium oleate and TOPSe precursors was used. Copper stearate is used as a source of copper. To build up the CdS shell, 0.2 ml of TOPS is used as a sulfur source. The synthesis process is conducted at a temperature of 180 °C for 5 min. This specific duration allows for the highest intensity of the exciton PL band and facilitates the incorporation of copper impurities.

2.1.2. $\mathcal{N}\ominus 2$ QDs

In the synthesis of CdSe quantum dots (QDs), specific proportions of surface stabilizers—hexadecylamine (HDA), tri-*n*-octylphosphine oxide (TOPO), and tri-*n*-octylphosphine (TOP)—were carefully selected to maximize the quantum yield (QY). This stabilizer mixture was selected for its ability to promote a controlled, slow nanoparticle growth rate and to minimize Ostwald ripening, thereby improving the uniformity and optical performance of the QDs. Previous studies [14,15] have demonstrated that this approach can achieve QY levels of up to 50–90 %. The synthesis was conducted with some modifications to the procedures outlined in Refs. [15–17]. The precursor ratio of cadmium to selenium (Cd:Se) was maintained at 1:5. The reaction was performed at 240 °C using a stabilizer ratio of TOP:O:HDA:TOP set to 66:33:1. This ratio was fine-tuned to maximize the luminescence efficiency and enhance the stability of the synthesized QDs.

2.1.3. $\mathcal{N}\ominus 3$ nc-QDs

A nanocomposite based on CdSe/CdS quantum dots was created by dispersing 0.25 mL of a CdSe/CdS QD solution (in heptane) into a matrix of polymethyl

methacrylate (PMMA). For this, 120–150 mg of technical-grade PMMA was initially dissolved in 1 mL of toluene. The resulting solution was stirred continuously until the PMMA was fully dissolved and all air bubbles were removed.

The nanocomposite mixture was then evenly applied to a clean microscope slide, allowing the solvent to evaporate rapidly. After the initial evaporation, the sample was left at room temperature for 24 h for complete stabilization. The preparation of the nanocomposite film was conducted in open air under natural daylight conditions. This method resulted in a homogeneous and stable film suitable for subsequent optical and structural analyses.

3. Results and discussion

3.1. Energy-dispersive X-ray spectra

Fig. 1 presents SEM, EDS, and elemental mapping images of the samples. The SEM images were taken at 800 \times magnification with a scale bar of 50 μ m. The EDS analysis results for sample $\mathcal{N}\ominus 1$ QDs are summarized in Table 1. The EDX analysis revealed atomic percentages of 49.78 % for Cd and 23.99 % for Se. The presence of (S) sulfur, which constitutes the shell material as sulfide, was also confirmed, with an atomic percentage of 0.51 % in the QDs. Additionally, these results confirm the proper distribution of cadmium and selenium within the structure.

As observed in the graphs of the $\mathcal{N}\ominus 1$ QDs samples, oxygen atoms were detected. This observation likely aligns with the model proposed in Ref. [23], where a cadmium-rich surface on the quantum dots (QDs) leads to the formation of a thin CdO layer. The high quantum yield of CdSe luminescence is attributed to the creation of this CdO layer, which results in a type-I core-shell structure. This structure helps passivate surface defects and effectively localize charge carriers.

For samples $\mathcal{N}\ominus 2$ QDs and $\mathcal{N}\ominus 3$ nc-QDs, the results of similar measurements are given in the Supplementary information (https://www.ephys.kz/cgi/viewcontent.cgi?filename=0&article=1247&context=journal&type=additional&preview_mode=1).

3.2. Absorption, luminescence (X-ray) and excitation spectra

Fig. 2 illustrates the optical absorption and photoluminescence (PL) spectra for the $\mathcal{N}\ominus 1$ and $\mathcal{N}\ominus 2$ QDs. The absorption spectrum reveals a distinct pattern typical of quantum confinement effects in semiconductor nanocrystals. At room temperature, the first absorption peak occurs at 549.2 nm, which corresponds to an energy of 2.26 eV (for $\mathcal{N}\ominus 1$ QDs, Fig. 2a).

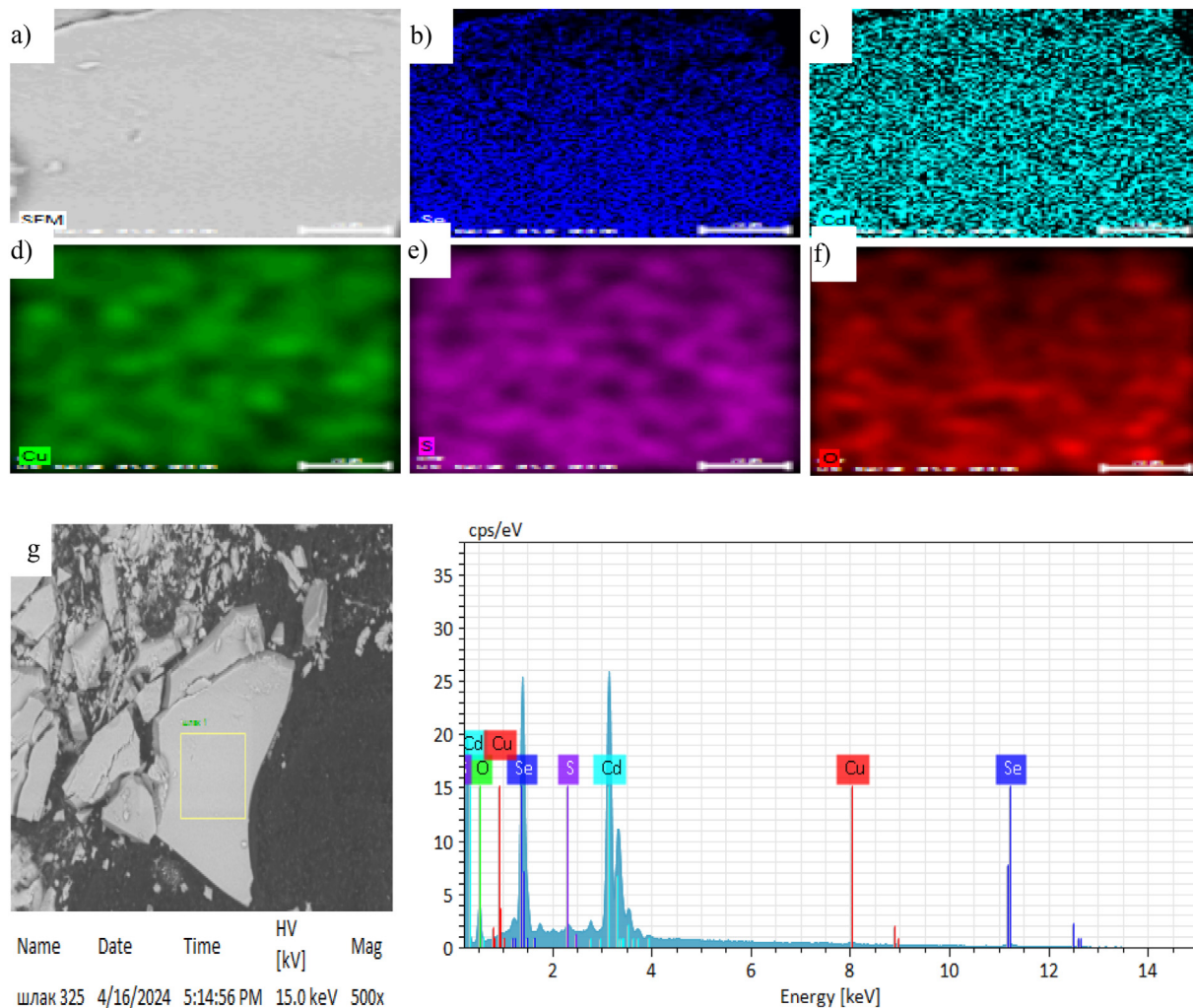


Fig. 1. SEM image (a); Element mapping (b, c, d, e, f); EDS spectra (g), of $N=1$ QDs.

Table 1. Results of the EDS analysis for $N=1$ QDs.

Element	At.No	Netto	Mass, %	Mass. norm, %	Atom, %	Abs., error % (1 sigma)	rel., error % (1 sigma)
O	8	3677	9.57	11.22	43.23	0.53	5.56
Se	34	34701	23.99	28.13	21.97	1.11	4.64
Cd	48	6016	49.78	58.36	32.02	1.36	2.73
Cu	29	495	1.44	1.69	1.64	0.16	10.79
S	16	1115	0.51	0.59	1.14	0.04	7.96
		Sum	85.29	100.00	100.00		

This peak is due to electronic transitions within the quantum-confined states of the QDs. When excited with 350 nm photons at room temperature, the PL spectrum shows a prominent emission band at 565.89 nm (2.19 eV), along with a weaker emission band in the longer-wavelength region.

The primary emission band exhibits a non-resonant Stokes shift of approximately 70 meV, which corresponds to the energy difference between the first absorption peak and the PL peak. This shift suggests

the involvement of electronic relaxation processes and the influence of surface states or defects. The quantum yield (QY) of the main PL band was determined to be 21.4 % using the comparative method, where the luminescence intensity of the sample was compared to that of a reference standard with a known QY—33 % for $N=1$ QDs. This moderate QY reflects the efficiency of radiative recombination processes within the QDs and the influence of surface passivation during synthesis.

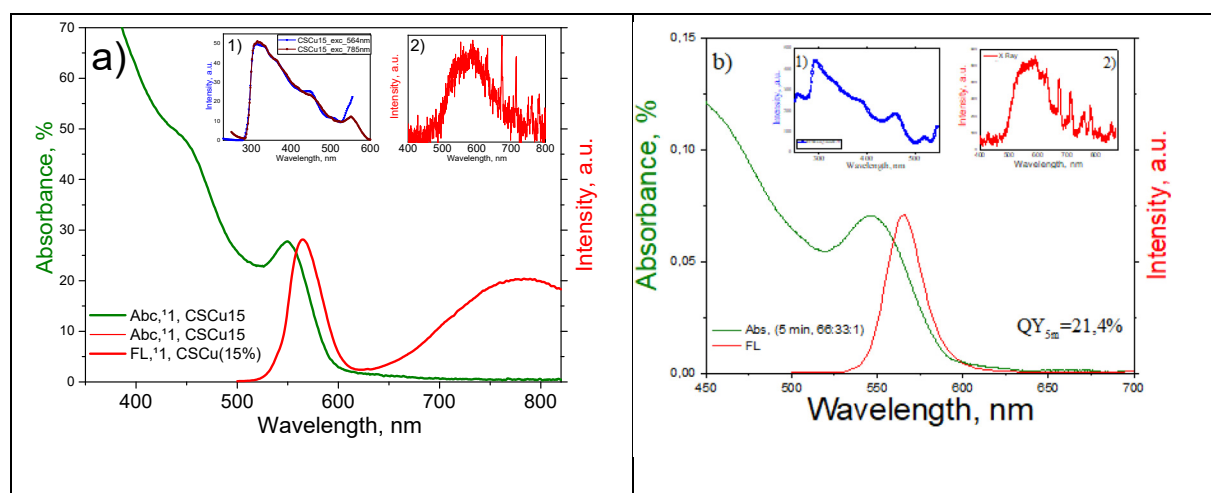


Fig. 2. Absorbance and photoluminescence spectra of: a) $N=1$ QDs; b) $N=2$ QDs (in the insert "blue" – excitation spectra, "red" - XRL) [24].

Fig. 2, inset (1), presents the excitation spectra of the quantum dot samples, while inset (2) shows the corresponding X-ray luminescence (XRL) spectra. Both sets of data were obtained at room temperature on a metallic substrate. The excitation spectra reveal a complex structure with several overlapping sub-bands, which reflects the size dispersion of the QDs and the resulting heterogeneity within the sample. Such a distribution in size contributes to the broadening and multiplicity of sub-bands within the excitation spectrum. These sub-bands represent distinct electron-hole transitions, which have been highlighted with vertical arrows of different colors, as described in Ref. [24]. The presence of these distinct excitation features underscores the influence of quantum confinement effects and size-dependent electronic transitions within the QDs.

The average size of the quantum dots was estimated using the wavelength of the first optical absorption peak. This calculation is based on the method described in Ref. [25], which establishes a relationship between absorption peak position and QD diameter. Relying on the principles of quantum confinement, this approach enables a reliable assessment of the nanoscale dimensions of the synthesized particles.

The spectral analysis of optical absorption and photoluminescence (PL) confirms typical quantum dot (QD) behavior, marked by pronounced excitonic absorption and sharp emission features. As noted in Ref. [26], similar results were obtained for CdSe QDs produced by the hot-injection method, where the emission was mainly attributed to band-edge transitions, with only a slight contribution from defect-related states.

The near-infrared (NIR) emission band is associated with defect-related states, most notably selenium vacancies, which, as highlighted in [ссылка], contribute significantly to this spectral feature [27,28]. These defect-related states serve as non-radiative

recombination centers, which can significantly impact the luminescence efficiency and spectral characteristics of QDs. The optical properties of quantum dots largely depend on the presence of defective states, which makes it particularly important to choose a synthesis method and approaches to surface passivation.

In contrast, the PL spectrum for CdSe/CdS QDs in a core-shell configuration demonstrates a single, well-defined emission band, indicative of effective surface passivation. As indicated in Ref. [27], the formation of a shell of wide-gap material, such as CDs, around the CdSe core contributes to a significant decrease in the density of surface defect states due to their passivation. This passivation eliminates the long-wavelength PL band typically associated with defect states, thereby enhancing the radiative recombination efficiency and narrowing the emission profile.

Further, a nanocomposite was fabricated from these QD samples, integrating the QDs into a polymer matrix. The PL and radioluminescence (RL) spectra of this nanocomposite were measured, providing insights into its optical properties and potential applications. The results clearly demonstrate that the passivation approach used in synthesis critically affects the formation of the spectral properties of the nanocomposite.

3.3. Time resolved spectroscopy

The effect of the structure on the spectral properties and dynamics of photoluminescence of CdSe/CdS, CdSe and nc-CdSe/CdS (nanocomposite) quantum dots was investigated. The samples were excited using a tunable YAG laser:Nd with a wavelength of 450 nm and a pulse duration of 5 ns, while the spectra were recorded in 3 ns increments. The photoluminescence spectra for samples No. 3 are shown in Fig. 3 (similar spectra for No. 1 can be found in additional materials).

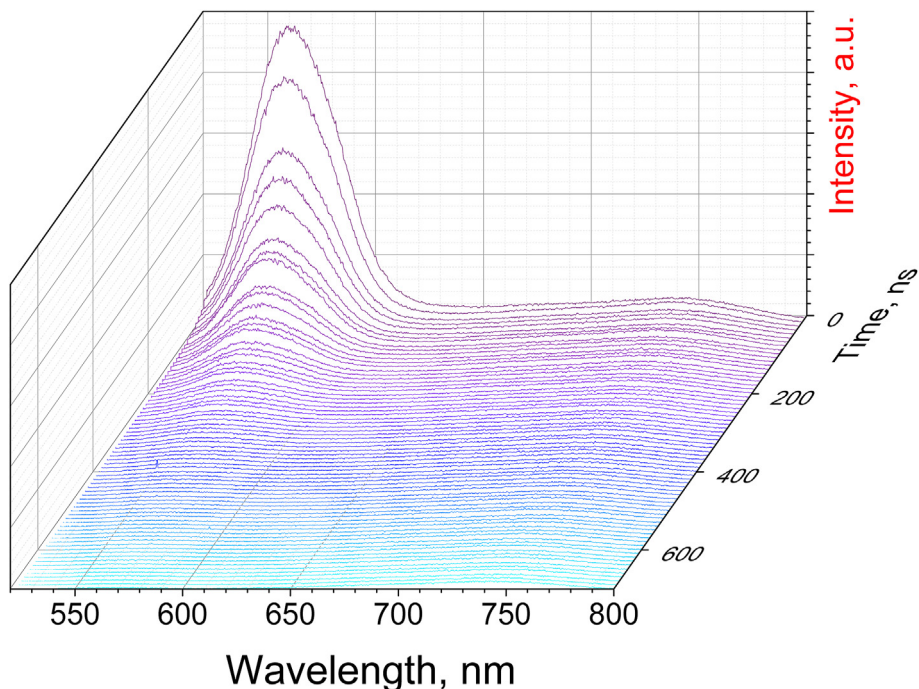


Fig. 3. Dynamics of luminescence of samples excited by a YAG:Nd laser with a wavelength of 450 nm and a pulse duration of 5 ns: a) $N^{\circ}3$ nc-QDs.

All spectra show a band with a maximum in the region of 550 nm, which corresponds to the radioactive recombination of excitons. In the photoluminescence spectrum of quantum dots, in addition to the exciton band, a long-wavelength band with a maximum of 742 nm is observed, due to defects on the surface of quantum dots, such as vacancies of selenium atoms, which act as traps for charge carriers [29,30].

The kinetic study of photoluminescence provides valuable insight into the recombination mechanisms and dynamic behavior of charge carriers in quantum dot systems. As illustrated in Fig. 4, the temporal evolution of photoluminescence intensity for all

investigated quantum dots, including both the excitonic band (~ 550 nm) and the defect-related band (~ 742 nm), can be accurately described by a tri-exponential decay model of the form (see Fig. 5):

$$A(t) = A_0 + \sum_i^3 A_i \exp\left(-\frac{t}{\tau_i}\right).$$

Here, A_i and τ_i represent the amplitude and lifetime of the i -th recombination channel, respectively. This approach assumes the coexistence of multiple independent radiative and non-radiative recombination

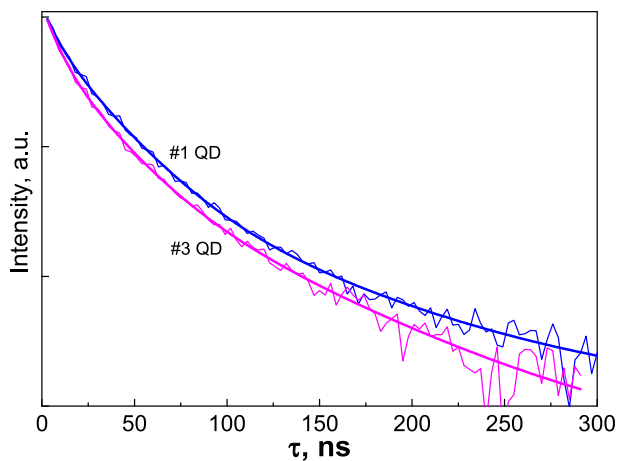


Fig. 4. Photoluminescence decay kinetics of $N^{\circ}1, 3$ nc-QDs.

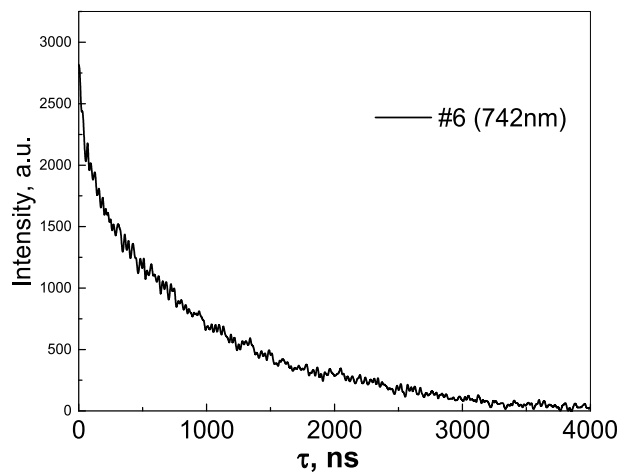


Fig. 5. Decay kinetics of FL $N^{\circ}3$ nc-QDs at 742 nm.

Table 2. Spectrum characteristics and decay times of fast and slow photoluminescence components.

Sample	d (nm)	Eg, eV [30]	λ_{max} (nm)	τ_1 , (ns)	τ_2 , (ns)	τ_3 , (ns)	$\langle\tau\rangle$, ns
$\mathcal{N}\ominus 1$ QDs	3.0	2.29	566	7	25	80	35
$\mathcal{N}\ominus 3$ nc-QDs	2.92	2.32	561	23	73	216	103
			740	21	151	1068	1033

pathways, typically associated with: fast component (τ_1) — direct band-edge (excitonic) recombination, intermediate component (τ_2) — recombination involving shallow surface states, slow component (τ_3) — carrier trapping and delayed emission from deep defect states or charge transfer interactions with the matrix. The individual decay components were extracted via multi-exponential fitting of the kinetic PL curves, and the corresponding parameters are summarized in Table 2.

To compare the overall recombination dynamics across different samples, the average photoluminescence lifetime $\langle\tau\rangle$ was calculated using the amplitude-weighted formula

$$\langle\tau\rangle = \frac{\sum_i^3 A_i \tau_i^2}{\sum_i^3 A_i \tau_i}.$$

This expression reflects the effective relaxation time considering the relative contribution and weight of each component.

In [31], the fluorescence of CdSe quantum dots (QDs) exhibits a tri-exponential decay with lifetimes of 57.39, 7.82, and 0.96 ns. The lifetimes of each recombination process decreased with the growth of the CdS shell, with the fastest transition contributing most significantly to the overall fluorescence. In our study, we demonstrated that the components of exciton relaxation differ between various types of QDs: CdSe “core” and CdSe/CdS “core-shell” structures. CdSe QDs exhibited a relaxation time of 27 ns. With the growth of the solid-state CdS shell and the corresponding increase in the size of CdSe/CdS QDs, the relaxation time changed only slightly, decreasing to 26 ns (Table 2). This suggests that the formation of the shell stabilizes exciton transitions, and the increase in size does not substantially influence the temporal component of exciton pair decay.

As Table 2 illustrates, an increase in the optical bandgap, calculated based on the formula from Ref. [31], correlates with a longer average PL relaxation time for smaller quantum dots (QDs). This effect has also been observed by other researchers [32]. For sample $\mathcal{N}\ominus 3$, the creation of the nanocomposite caused a notable rise in exciton lifetime, reaching 103 ns. This can be explained by the disruption of QD crystallinity

and the effect of the polymer matrix on the QD surface, which likely stabilizes surface states and minimizes non-radiative recombination. Additionally, the PL spectrum of the nano composite contains a weak intensity band at 720 nm, with a decay time of 1.033 μs . This emission band is related to surface defects in the QD crystal structure or the formation of a long-wavelength band resulting from the incorporation of copper ions. These copper ions introduce energy levels within the forbidden band of CdS, as described in related studies [27].

Thus, the study demonstrates that structural modifications of quantum dots, such as the formation of a CdS shell and the creation of nanocomposites, significantly affect the exciton relaxation processes and the temporal characteristics of photoluminescence. The growth of the CdS shell contributes to the stabilization of exciton transitions and shifts the dominant contribution towards faster recombination processes, while the increase in nanoparticle size has a negligible effect on the overall exciton lifetime. The introduction of a nanocomposite matrix, in turn, significantly increases the exciton lifetime by reducing non-radiative recombination due to the stabilization of surface states. The presence of an additional long-wavelength luminescence band is associated with surface defects or copper impurities, which underscores the importance of controlling chemical composition and structure to manage the optical properties of quantum dots.

4. Conclusions

In this study, we successfully synthesized color-tunable cadmium selenide (CdSe) QDs and characterized their optical and structural properties. At room temperature, time-resolved fluorescence spectroscopy was employed to explore charge carrier relaxation and transfer mechanisms in CdSe and CdSe/CdS core-shell quantum dots. The study demonstrated a noticeable reduction in emission lifetimes for CdSe QDs after the formation of a CdS shell. This suggests that the CdS shell plays a crucial role in strengthening carrier confinement and reshaping the recombination dynamics within the nanostructure.

A comprehensive study was conducted on the static and time-resolved luminescent properties of colloidal CdSe quantum dots (QDs), focusing on the effects of ligand composition, structural architecture, and surface

engineering. Synthesis protocols were refined to boost quantum yield at ambient conditions, leading to QDs with superior optical characteristics. The impact of structural modifications on emission spectra and photoluminescence dynamics was thoroughly examined for three systems: pure CdSe QDs, CdSe/CdS core–shell configurations, and polymer-based composites containing CdSe QDs.

As depicted in the presented luminescence decay profiles were found to be highly sensitive to surface modifications and QD size. Specifically, an increase in QD diameter resulted in a marked decrease in luminescence decay times, consistent with the size-dependent quantum confinement effects in colloidal QDs. The integration of quantum dots into polymer matrices through non-covalent bonding has been shown to prolong exciton lifetimes on their surfaces. This improvement is largely attributed to the polymer's role in stabilizing surface electronic states and minimizing non-radiative recombination processes.

The study underscores the importance of tailoring structural and surface properties to achieve desired optical characteristics and excitonic dynamics in QDs. The insights gained from this study play an important role in advancing the design of quantum dots for high-performance optoelectronic devices, such as light-emitting diodes, laser sources, and biomedical imaging systems. The observed enhancement in exciton lifetime through polymer encapsulation offers a promising avenue for improving the stability and performance of QD-based composites.

Funding

This research is funded by the Science Committee of Science of the Ministry of Science and Higher Education of the Republic of Kazakhstan (Grant No. AP 19676416).

Conflict of interest

The authors have no relevant financial or non-financial interests to disclose.

References

- [1] T. Trindade, P. O'Brien, N.L. Pickett, Nanocrystalline semiconductors: synthesis, properties, and perspectives, *Chem. Mater.* 13 (11) (2001) 3843–3858, <https://doi.org/10.1021/cm000843p>.
- [2] J.D. Bryan, D.R. Gamelin, Doped semiconductor nanocrystals: synthesis, characterization, physical properties, and applications, *Prog. Inorg. Chem.* 54 (2005) 47–126, <https://doi.org/10.1002/0471725569.ch2>.
- [3] A.M. Smith, S. Nie, Semiconductor nanocrystals: structure, properties, and band gap engineering, *Acc. Chem. Res.* 43 (2) (2010) 190–200, <https://doi.org/10.1021/ar9001069>.
- [4] Y. Al-Douri, M.M. Khan, J.R. Jennings, Synthesis and optical properties of II–VI semiconductor quantum dots: a review, *J. Mater. Sci. Mater. Electron.* 34 (2023) 993, <https://doi.org/10.1007/s10854-023-10435-5>.
- [5] O. Stroyuk, O. Raievska, D.R.T. Zahn, C.J. Brabec, Exploring highly efficient broadband self-trapped-exciton lumino-phors: from 0D to 3D materials, *Chem. Eur. J.* 24 (2024) e202300241, <https://doi.org/10.1002/tcr.202300241>.
- [6] S.K. Goswami, T.S. Kim, E. Oh, K.K. Challa, E.T. Kim, Optical properties and effect of carrier tunneling in CdSe colloidal quantum dots: a comparative study with different ligands, *AIP Adv.* 2 (3) (2012) 032132, <https://doi.org/10.1063/1.4745080>.
- [7] Y. Qu, L. Zhang, L. An, H. Wei, Investigation on photoluminescence quenching of CdSe/ZnS quantum dots by organic charge transporting materials, *Mater. Sci. Pol.* 33 (4) (2015) 709–713, <https://doi.org/10.1515/msp-2015-0120>.
- [8] H.W. Park, D.H. Kim, Intense visible luminescence in CdSe quantum dots by efficiency surface passivation with H₂O molecules, *J. Nanomater.* 2012 (2012) 892506, <https://doi.org/10.1155/2012/892506>.
- [9] S.R. Cordero, P.J. Carson, R.A. Estabrook, G.F. Strouse, S.K. Buratto, Photo-activated luminescence of CdSe quantum dot monolayers, *J. Phys. Chem. B* 104 (51) (2000) 12137–12142, <https://doi.org/10.1021/jp001771s>.
- [10] A. Kumari, R.R. Singh, Encapsulation of highly confined CdSe quantum dots for defect-free luminescence, *Phys. E Low-dimens. Syst. Nanostruct.* 89 (2017) 77–85, <https://doi.org/10.1016/j.physe.2017.01.031>.
- [11] D. Simonot, C. Roux-Byl, X. Xu, W. Daney de Marcillac, C. Dabard, M.G. Silly, et al., Optical and X-ray photo-emission spectroscopies of core/shell colloidal CdSe/CdS quantum dots: modeling and experimental determination of band alignment, *arXiv preprint arXiv:2406.17366* (2024), <https://doi.org/10.48550/arXiv.2406.17366>.
- [12] Z. Ning, M. Molnár, Y. Chen, P. Friberg, L. Gan, H. Ågren, Y. Fu, Role of surface ligands in optical properties of colloidal CdSe/CdS quantum dots, *Phys. Chem. Chem. Phys.* 13 (13) (2011) 5848–5854, <https://doi.org/10.1088/1757-899X/562/1/012067>.
- [13] Z. Liu, C. Chang, W. Zhang, M. Yang, Q. Zhang, Research on ligand properties of CdSe quantum dots, *IOP Conf. Ser. Mater. Sci. Eng.* 562 (2019) 012067, <https://doi.org/10.1088/1757-899X/562/1/012067>.
- [14] I. Mekis, D.V. Talapin, A. Kornowski, M. Haase, H. Weller, One-pot synthesis of highly luminescent CdSe/CdS core–shell nanocrystals via organometallic and “greener” chemical approaches, *J. Phys. Chem. B* 107 (30) (2003) 7454–7462, <https://doi.org/10.1021/jp0278364>.
- [15] D.V. Talapin, A.L. Rogach, A. Kornowski, M. Haase, H. Weller, Highly luminescent monodisperse CdSe and CdSe/ZnS nanocrystals synthesized¹ in a hexadecylamine–triethylphosphine oxide–triethylphosphine mixture, *Nano Lett.* 1 (4) (2001) 207–211, <https://doi.org/10.1021/nl0155126>.
- [16] L. Qu, X. Peng, Control of photoluminescence properties of CdSe nanocrystals in growth, *J. Am. Chem. Soc.* 124 (9) (2002) 2049–2055, <https://doi.org/10.1021/ja017002j>.
- [17] C. de Mello Donegá, R. Koole, A. Meijerink, D. Vanmaekelbergh, Size- and shape-dependent luminescence of CdSe quantum dots, *J. Phys. Chem. B* 107 (19) (2003) 489–496, <https://doi.org/10.1103/PhysRevB.71.201307>.
- [18] Y. Ben-Shahar, D. Stone, U. Banin, Rich landscape of colloidal semiconductor–metal hybrid nanostructures: synthesis, synergetic characteristics, and emerging applications, *Chem. Rev.* 123 (6) (2023) 3790–3851, <https://doi.org/10.1021/acs.chemrev.2c00770>.
- [19] H.A. Nguyen, G. Dixon, F.Y. Dou, S. Gallagher, S. Gibbs, D.M. Ladd, et al., Design rules for obtaining narrow luminescence from semiconductors made in solution, *Chem. Rev.* 123 (12) (2023) 7890–7952, <https://doi.org/10.1021/acs.chemrev.3c00097>.
- [20] H. Xu, V. Chmyrov, J. Widengren, H. Brismar, Y. Fu, Mechanisms of fluorescence decays of colloidal CdSe–CdS/ZnS quantum dots unraveled by time-resolved fluorescence measurement, *Phys. Chem. Chem. Phys.* 17 (41) (2015) 27588–27595, <https://doi.org/10.1039/C5CP03109E>.

- [21] P.N. Tananaev, S.G. Dorofeev, R.B. Vasilev, T.A. Kuznecova, Poluchenie nanocrystallov CdSe legirovannogo medyu, Neorg. Mater. T.45 (4) (2009) S.393–S.398.
- [22] D.V. Talapin, I. Mekis, S. Gotzinger, A. Kornowski, O. Benson, H. Weller, CdSe/CdS/ZnS and CdSe/ZnSe/ZnS core–shell–shell nanocrystals, *J. Phys. Chem. B* 108 (49) (2004) 18826–18831, <https://doi.org/10.1021/jp046481g>.
- [23] K.B. Subila, G.K. Kumar, S.M. Shivaprasad, K.G. Thomas, Luminescence properties of CdSe quantum dots: role of crystal structure and surface composition, *J. Phys. Chem. Lett.* 4 (16) (2013) 2774–2779, <https://doi.org/10.1021/jz401198e>.
- [24] R.C. Keitel, R. Brechbühler, A. Cocina, F.V. Antolinez, S.A. Meyer, S.J.W. Vonk, et al., Fluctuations in the photoluminescence excitation spectra of individual semiconductor nanocrystals, *J. Phys. Chem. Lett.* 15 (12) (2024) 4844–4850, <https://doi.org/10.1021/acs.jpcllett.4c00516>.
- [25] W.W. Yu, L. Qu, W. Guo, X. Peng, Experimental determination of the extinction coefficient of CdTe, CdSe, and CdS nanocrystals, *Chem. Mater.* 15 (14) (2003) 2854–2860, <https://doi.org/10.1021/cm034081k>.
- [26] W.W. Yu, X. Peng, Formation of high-quality CdS and other II–VI semiconductor nanocrystals in noncoordinating solvents: tunable reactivity of monomers, *Angew. Chem. Int. Ed.* 41 (13) (2002) 2368–2371, [https://doi.org/10.1002/1521-3773\(20020703\)41:13<2368::AID-ANIE2368>3.0.CO;2-G](https://doi.org/10.1002/1521-3773(20020703)41:13<2368::AID-ANIE2368>3.0.CO;2-G).
- [27] G. Güleroğlu, C. Ünlü, Spectroscopic investigation of defect-state emission in CdSe quantum dots, *Turk. J. Chem.* 45 (2) (2021) 520–527, <https://doi.org/10.3906/kim-2101-66>.
- [28] R.W. Meulenberg, T. van Buuren, K.M. Hanif, T.M. Willey, G.F. Strouse, L.J. Terminello, Structure and composition of Cd-doped CdSe nanocrystals using soft X-ray absorption spectroscopy, *Nano Lett.* 4 (11) (2004) 2277–2285, <https://doi.org/10.1021/nl048738s>.
- [29] L.A. Golovan', A.V. Yelopov, V.B. Zaitseva, A.A. Ezhova, D.M. Zhigunov, O.N. Karpov, G.A. Shandryuk, A.S. Merekalov, R.V. Talroze, Photoluminescence of CdSe and CdSe/ZnS quantum dots in amorphous and liquid-crystalline polymer matrices, *Polym. Sci.* 62 (6) (2020) 430–443, <https://doi.org/10.31857/S2308112020060048>.
- [30] Z. Ji, Z. Song, Exciton radiative lifetime in CdSe quantum dots, *J. Semiconduct.* 44 (3) (2023) 032702, <https://doi.org/10.1088/1674-4926/44/3/032702>.
- [31] R. Beaulac, P.I. Archer, S.T. Ochsenein, D.R. Gamelin, Mn²⁺-doped CdSe quantum dots: new inorganic materials for spin-electronics and spin-photonics, *Adv. Funct. Mater.* 18 (24) (2008) 3873–3891, <https://doi.org/10.1002/adfm.200801016>.
- [32] K. Gong, J.E. Martin, L.E. Shea-Rohwer, P. Lu, D.F. Kelley, Radiative lifetimes of zincblende CdSe/CdS quantum dots, *J. Phys. Chem. C* 119 (4) (2015) 2239–2249, <https://doi.org/10.1021/jp5118932>.